Journal of Ethnopharmacology and Toxicology
Research Article

Computational screening of phytochemicals as DPP-4 inhibitors for treating type 2 diabetes

Ananta Swargiary[1*], Arup Swargiary[1], Beauty Narzary[1], Kalyan Dey[2], Dulur Brahma[1]

[1]Pharmacology and Bioinformatics Laboratory, Department of Zoology, Bodoland University, Kokrajhar, 783370, India.
[2]Department of Physics, Bodoland University, Kokrajhar, 783370, India.

[*]**Correspondence**
Ananta Swargiary
ananbuzoo101@gmail.com

Volume: 2, Issue: 2, Pages: 44-55
DOI: https://doi.org/10.37446/jet/rsa/2.2.2024.44-55
Received: 25 August 2024 / Accepted: 18 October 2024 / Published: 31 December 2024

Dipeptidyl peptidase-4 (DPP4) is an enzyme responsible for degrading incretin hormones, which are key regulators of insulin secretion and blood glucose levels. Inhibition of DPP4 prolongs incretin activity, thereby enhancing glycemic control and offering therapeutic benefits in the management of Type 2 diabetes mellitus (T2DM). Although synthetic DPP4 inhibitors are commonly used, plant-based compounds present a promising and potentially safer alternative. This study aimed to evaluate the DPP4 inhibitory potential of plant-derived compounds through *in silico* approaches, including molecular docking, molecular dynamics (MD) simulations, and ADMET (absorption, distribution, metabolism, excretion, and toxicity) analysis. Among the screened compounds, Apigenin 7-O-methylglucuronide, a bioactive molecule, exhibited a higher binding affinity to DPP4 (-9.1 kcal/mol) compared to sitagliptin (-8.43 kcal/mol), a standard DPP4 inhibitor. Furthermore, MD simulations over 100 ns demonstrated greater stability of the Apigenin 7-O-methylglucuronide–DPP4 complex relative to the sitagliptin–DPP4 complex. ADMET profiling revealed favorable pharmacokinetic properties, including high oral bioavailability and minimal inhibition of cytochrome P450 enzymes. These findings underscore the potential of Apigenin 7-O-methylglucuronide as a natural DPP4 inhibitor and support its further investigation as a candidate for alternative T2DM therapies.

Keywords: *Dipeptidyl peptidase-4 inhibitor, apigenin 7-O-methylglucuronide, molecular docking, molecular dynamics simulation, type 2 diabetes*

Introduction

Diabetes mellitus (DM) is a global health issue characterized by chronic hyperglycemia, leading to organ damage, including the eyes, kidneys, heart, nerves, and blood vessels. It results from impaired insulin secretion or action (American Diabetes Association, 2014; Alam et al., 2014). In 2014, 366 million people had DM, with this number projected to reach 552 million by 2030[2]. Type-2 DM, the most common form, accounts for over 90% of adult cases (Kharroubi and Darwish, 2015). Type 1 diabetes results from the destruction of insulin-producing cells, while T2DM is marked by insulin resistance, reduced insulin production, and β-cell failure, impairing glucose transport (Robertson, 1995; Khan, 2014; Olokoba et al., 2012). Genetic predisposition and lifestyle factors such as inactivity, smoking, and alcohol consumption play key roles in T2DM (Manson et al., 2001). Conditions like obesity, hypertension, and chronic diseases can further trigger or worsen it (Alberti et al., 2005; Powers, 2005). Insulin therapy effectively regulates blood sugar levels and reduces diabetic complications (Swinnen et al., 2009; Swargiary et al., 2024). However, it has limitations, including weight gain and a higher risk of hypoglycemia. Various pharmacological agents, such as sulfonylureas, biguanides, meglitinides, thiazolidinediones, alpha-glucosidase inhibitors, sodium glucose transporter-2 inhibitors, and DPP4 inhibitors, are available to manage hyperglycemia, each with distinct mechanisms of action (Al-Saleh et al., 2021). One effective approach to managing hyperglycemia is targeting dipeptidyl peptidase-4, an enzyme that rapidly degrades incretin

hormones, such as glucagon-like peptide-1 and glucose-dependent insulinotropic polypeptide. These hormones play a critical role in enhancing insulin secretion, suppressing glucagon release, and regulating blood glucose levels. By inhibiting DPP4, DPP4 inhibitors prolong the activity of incretins, thereby improving glycemic control without a significant risk of hypoglycemia. This mechanism makes them a valuable therapeutic option, especially for patients with T2DM (Deacon, 2020). Although synthetic DPP4 inhibitors are available, their long-term safety remains uncertain, prompting the search for alternative drugs. Bioactive compound -based DPP4 inhibitors offer a potentially safer option, with studies highlighting their inhibitory effects (Yang et al., 2020). Identifying key bioactive compounds with DPP4 inhibitory activity is essential for developing effective diabetes treatments. Therefore, this study aims to evaluate the DPP4 inhibition potential of selected bioactive compound through molecular docking, molecular dynamics simulation, and free energy analysis. Additionally, the study assesses their drug-likeness and investigates their toxicity profiles using ADMET analysis.

Materials and Methods

Collection and preparation of phytochemicals

Phytochemicals with DPP4 inhibitory activity were selected from research articles using databases like Google, Google Scholar, and PubMed, with keywords such as "DPP4 inhibitor plant compounds," "phytocompounds with DPP4 inhibition properties," and "DPP4 inhibitor phytocompounds." Their sdf formats were retrieved from the PubChem database (https://www.ncbi.nlm.nih.gov), and the sdf format of DPP4 inhibitors was obtained from the DrugBank database (https://go.drugbank.com). All compounds were then converted to pdbqt file format using OpenBabe (O'Boyle et al., 2011) and AutoDock Tools (Trott and Oslon, 2010).

Preparation of receptor (DPP4) and active pocket prediction

The DPP4 protein structure with vildagliptin (PDB ID: 6B1E) was downloaded from the Protein Data Bank (https://www.rcsb.org/) and processed using Biovia Discovery Studio. Water molecules were removed, polar hydrogens and Gasteiger charges were added, and the pdb file was converted to pdbqt format using AutoDock Tools 1.5.6. The active site, consisting of 14 residues, was defined using the PrankWeb platform, a machine learning-based method for prediction of ligand binding sites from protein structure (Jakubec et al., 2022). The grid box was set at coordinates 38.350, 51.154, and 37.154 with dimensions 60 × 62 × 58. Grid box was prepared by AutoDock Tools by selecting the amino acid residues as predicted by the PrankWeb platform (Swargiary et al., 2024).

Pharmacokinetics and ADMET analysis

A total of 84 phytochemicals and FDA-approved reference drugs were evaluated for drug-likeness based on Lipinski's Rule of Five (Lipinski, 2004), analyzing properties such as molecular weight, hydrogen bond donors/acceptors, and LogP. Pharmacokinetic properties, including absorption, distribution, metabolism, excretion, and toxicity (ADMET), were predicted using pkCSM (Pires et al., 2015), SwissADME (Lipinski, 2004), and ADMETlab (Xiong et al., 2021).

Molecular docking (MD)

Molecular docking was done using AutoDock Vina on a system with Windows 10, 8 GB RAM, and 1 TB memory. The docking was repeated three times for all phytochemicals and reference drugs. The results were compared with four FDA-approved drugs: alogliptin, saxagliptin, sitagliptin, and vildagliptin. The ligand was then combined with DPP4 using PyMOL-1.7.4.5 Schrödinger software, and docking complexes were visualized with Biovia Discovery Studio Visualizer-2021.

Molecular dynamics simulation study

Phytochemicals and reference drugs with the strongest binding energies were further investigated using Molecular Dynamics Simulation (MDS) to assess binding stability and dynamics. MDS was performed with Gromacs-2023.2 (Abraham et al., 2015; Velan et al., 2021) on a workstation running Ubuntu-22.04.3 LTS, equipped with 32 GB RAM, an RTX-4060 Ti GPU, and 4 TB storage. The CHARMM-27 force field and TIP3P water model were used, with solvation achieved via Na+ and Cl- ions. Ligand parameters were prepared using UCSF Chimera 1.17.1 (Petterson et al., 2004) and the SwissParam Server (Zoete et al., 2011). DPP4 structure optimization included Gasteiger charges via Chimera's DockPrep function. The system underwent 100 ps equilibration before a 100 ns MD run. Post-MD analysis included root

mean square deviation (RMSD), root mean square fluctuations (RMSF), radius of gyration (Rg), hydrogen bond dynamics, and energy fluctuations, with graphical outputs generated using QtGrace software.

Molecular Mechanics/ Poisson Boltzmann Surface Area (MM/PBSA) Analysis

Binding free energies of selected DPP4 and ligand complexes were estimated using the MM/PBSA package (Kumari and Kumar, 2014; Valdes et al., 2021). The calculation included components such as binding free energy (-kcal/mol), van der Waals energy (VDWAALS), electrostatic energy (EEL), polar solvation energy (EPB), non-polar solvation energy (ENpolar), and total energy changes. The following equation was used to compute the binding free energy of the protein-ligand complexes:

$$\Delta G_{bind}\ (MM/PBSA) = G_{complex} - (G_{receptor} + G_{ligand})$$

Where, $G_{complex}$ represents the total binding free energy of the complex, and $G_{receptor}$ and G_{ligand} depict the total free energies of the isolated protein and ligand in the solvent, respectively.

Statistical analysis

All calculations were carried out in Microsoft Excel. Molecular docking was carried out for three replicates for each bioactive compound (n = 3) and values are expressed as mean ± standard deviation.

Results

Structural analysis of protein

The DPP4 protein, consisting of 766 amino acids, exhibits a variety of secondary structures, including coils, sheets, helices, and turns (Figure 1a) and detailed data is provided as Supplementary File 1. The longest coil consists of 14 amino acid residues and the longest sheet consists of 11 residues. The longest helix stretches over 18 amino acids. Coil structures were found to be more prevalent than other structures, occurring 79 times, followed by turns (51), sheets (46), and helices (18 times). The predominance of coils suggests their significant role in the protein's overall structure and function. Figure 1 illustrates the 3D structure of the DPP4 protein, the Ramachandran plot, and sequence alignments. The Ramachandran plot (Figure 1b) reveals that 97.25% of the amino acid residues are positioned within the favored region, indicating good stereochemical quality. Additionally, no bad bonds or bond angles were detected, confirming the structural integrity of the protein. Around 1.50% of residues were identified as Ramachandran outliers, with a clash score of 1.22, suggesting minimal steric conflicts. This structural information highlights the overall stability and quality of the DPP4 model, which is crucial for understanding its biological function.

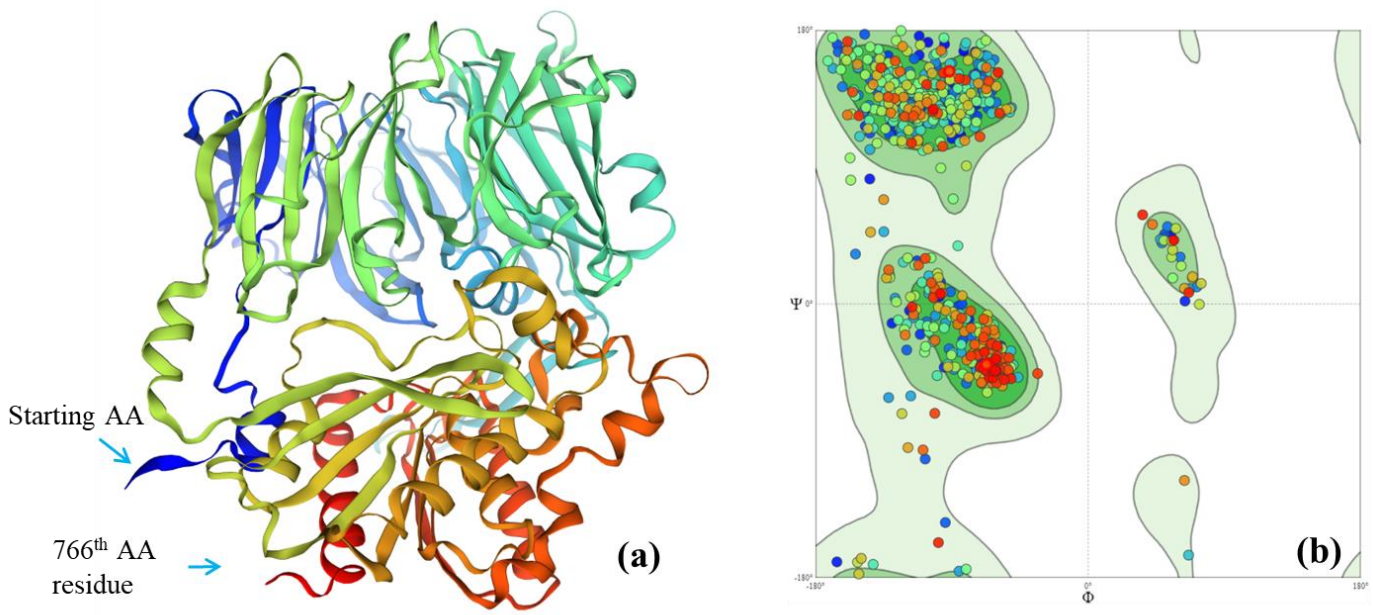

Figure 1. Structural analysis of DPP4 protein. (a) 3D structure of DPP4, and (b) Ramachandran Plot of protein

Drug-likeness and ADMET study

All 84 bioactive compounds and four FDA-approved drugs were screened for drug-likeness, including Lipinski's Rule of Five (Supplementary File 2). While all reference drugs adhered to the rule, the top five bioactive compounds with the highest docking scores violated the rule and therefore were rejected for further study. FDA-approved drugs had complexity scores below 650, whereas 37 compounds exceeded 700. Reference drugs contained fewer than 30 heavy atoms, while some phytochemicals, such as rugosin A (79 atoms), had significantly more. LogP values for reference drugs ranged from 0.6 to 0.9, while bioactive compounds varied widely (-2.9 to 13.3). Phytochemicals also showed greater diversity in hydrogen bond donors, acceptors, and rotatable bonds. The topological polar surface area (TPSA) ranged from 20.2 to 611.5 Å², compared to 76.4 to 93.7 Å² for reference drugs. Molecular weights of FDA-approved drugs were below 500 g/mol, whereas some compounds, such as rugosin A, exceeded 1000 g/mol. However, lower molecular weight phytochemicals generally exhibited weaker binding affinity for DPP4.

Apigenin 7-O-methylglucuronide, which adhered to Lipinski's rule, and Sitagliptin, the highest-scoring reference drug, were further evaluated for ADMET properties (Figure 2). The study observed that the reference drug sitagliptin showed superior human intestinal absorption (0.766) compared to A7OM (0.323) and had a lower plasma protein binding affinity (74.85%) than A7OM (79.2%), indicating better therapeutic potential. Sitagliptin also exhibited higher blood-brain barrier permeability (0.961) than A7OM (0.046). Both compounds had moderate to low interactions with cytochrome-P450 enzymes, suggesting favorable metabolism. Sitagliptin had a shorter half-life (1.218 h) than A7OM (1.48 h), while A7OM displayed a slightly higher clearance rate (1.252 ml/min). The LD_{50} of A7OM was 500.18 mg/kg, higher than the reference drug sitagliptin (292.37 mg/kg), suggesting lower toxicity for A7OM.

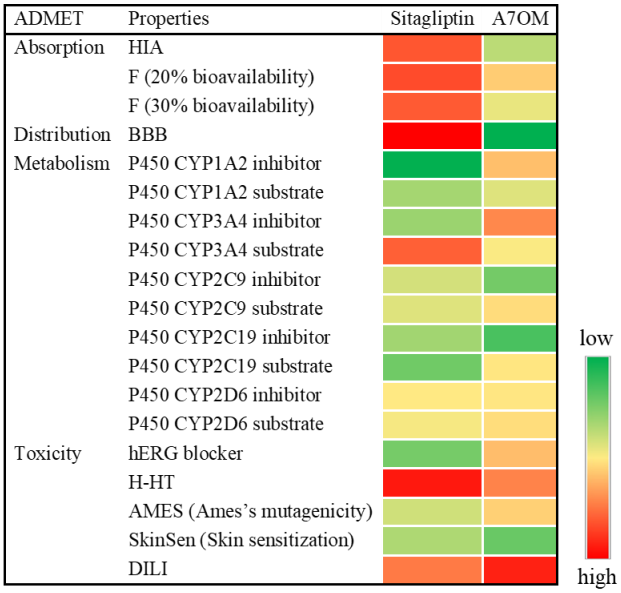

Figure 2. Heatmap of ADME properties of Apigenin 7-O-methylglucuronide (A7OM) and Sitagliptin

Phytochemicals and Molecular Docking

A total of 84 bioactive compounds were collected from the literature and docking scores of phytochemicals and reference drugs with the DPP4 protein is provided as Supplementary File 3. The average binding energies of the reference drugs (-7.92 kcal/mol) and bioactive compounds (-7.94 kcal/mol) were nearly identical. Among the reference drugs, sitagliptin showed the highest binding affinity (-8.43 ± 0.21 kcal/mol). Of the 84 bioactive compounds, robinin, eriocitrin, and rugosin A exhibited the strongest binding affinities (-10.4, -9.97, and -9.97 kcal/mol, respectively). These phytochemicals were isolated from *Lens culinaris* (Kim et al., 1998), *Citrus limon* (Fan et al., 2013), and *Rosa gallica* (Kato et al., 2016). Compounds with binding energies bigger than A7OM were excluded from further study due to the violation of Lipinski's rule. Figure 3 illustrates the 3D and 2D binding interactions of DPP4 with sitagliptin (Figure 3a, b) and A7OM (Figure 3c, d). Sitagliptin, the top-scoring reference drug, was selected for further analysis. Docking analysis revealed that van der Waals interactions dominated the sitagliptin-DPP4 complex, while hydrogen bonds were predominant in the DPP4-A7OM complex. Sitagliptin showed seven van der Waals interactions and four hydrogen bonds, while A7OM had five van der Waals interactions and four hydrogen bonds (Supplementary File 4). Additionally, three unfavorable interactions were detected in the DPP4-sitagliptin complex, compared to one in the DPP4-A7OM complex.

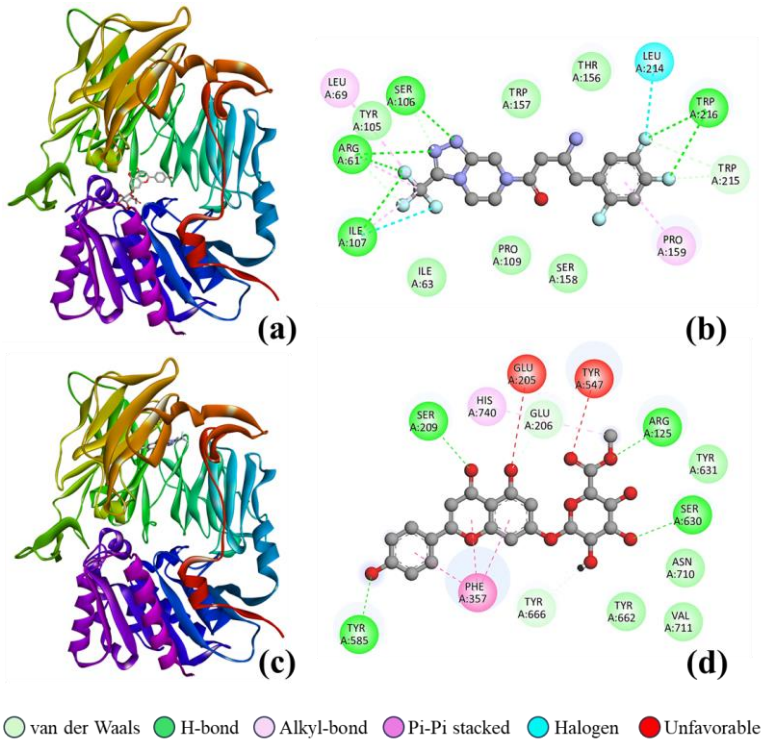

Figure 3. 3D and 2D display of binding interactions of reference drug Sitagliptin (a & b) and Apigenin 7-O-methylglucuronide (c & d) with DPP4 protein

Molecular dynamics simulation

Molecular dynamics simulations were performed to assess the stability and binding interactions of the DPP4-sitagliptin and DPP4-A7OM complexes. Ligand-receptor complexes with higher binding affinities than A7OM were excluded from further analysis due to non-compliance with Lipinski's Rule of Five, which predicts drug-likeness property based on the physicochemical properties. The stability of the DPP4 protein in both its apo and ligand-bound states was evaluated using structural and dynamic parameters, including RMSD, RMSF, Rg, hydrogen bonding (HB), and total energy fluctuations. These analyses provided valuable insights into the conformational stability, flexibility, and compactness of the protein throughout the simulation.

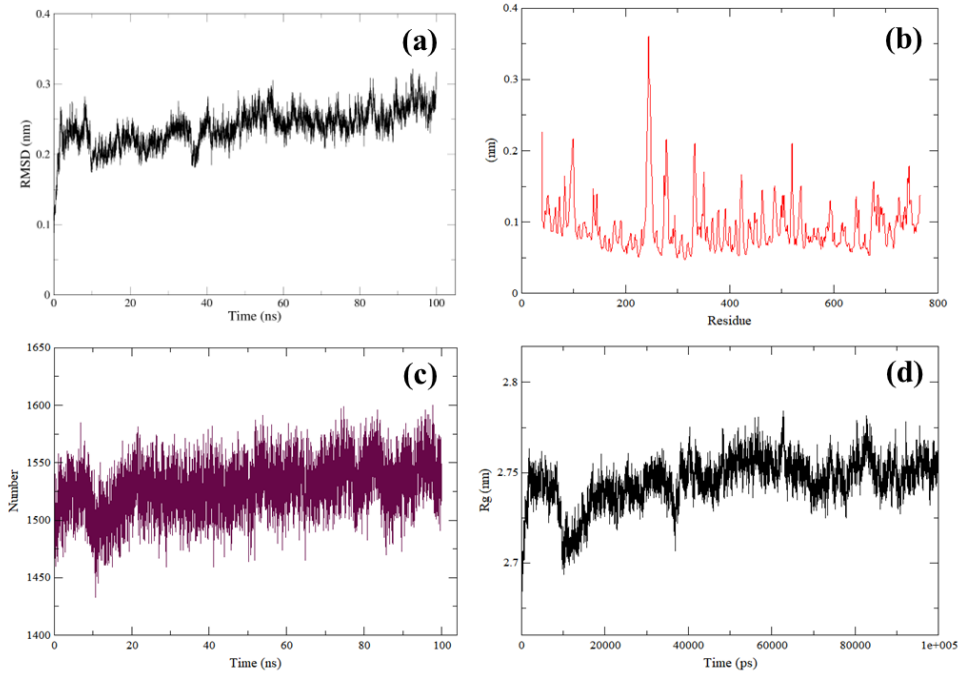

Figure 4. Parameters of MD Simulation of DPP4 apo-protein; (a) RMSD, (b) RMSF, (c) H-bonds, and (d) Rg (Radius of gyration)

Figure 4 depicts the stability analysis of the apo-protein. The RMSD remained stable at an average of 0.24 ± 0.02 nm, indicating minimal structural deviations throughout the 100 ns simulation (Figure 4a). The RMSF analysis revealed minor fluctuations localized between residues 200–300, likely corresponding to flexible loop regions, with a mean value of 0.09 ± 0.03 nm (Figure 4b). Hydrogen bonding analysis showed a high of ~1600 intramolecular bonds, demonstrating robust structural integrity (Figure 4c). Rg analysis further confirmed stable protein compactness with no significant deviations observed (Figure 3d).

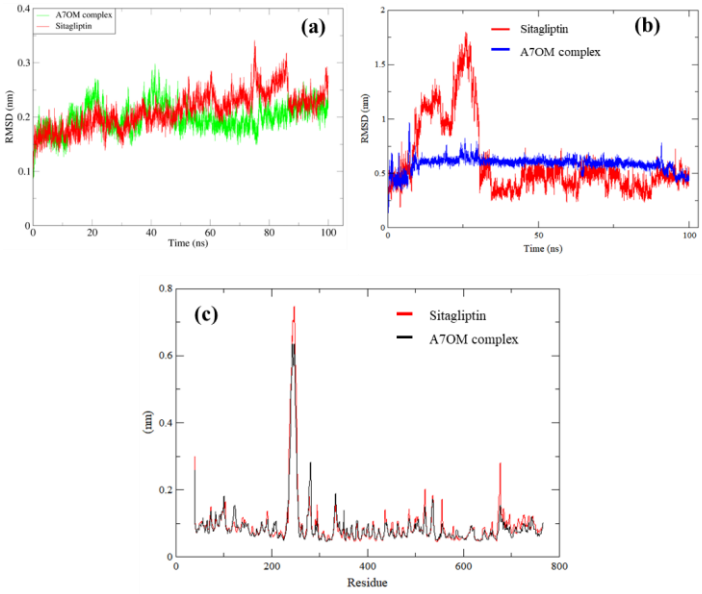

Figure 5. Conformational changes in the DPP4-ligand complexes; (a) RMSD of ligand bound complexes, (b) RMSD of ligands and (c) RMSF during simulation period

Lastly, total energy fluctuations remained stable during the simulation, supporting the overall structural stability of the apo-protein system (Figure 4e). Figure 5 illustrates the conformational changes in ligand-bound DPP4 complexes over 100 ns, including RMSD and RMSF analyses. The RMSD of the A7OM complex was slightly higher than the sitagliptin complex, while both were lower than the apo-protein (0.24 ± 0.03 nm), indicating increased stability upon ligand binding. The sitagliptin complex exhibited greater RMSD variation (0.21 ± 0.03 nm) compared to the A7OM complex (0.20 ± 0.02 nm), suggesting better binding stability for A7OM (Figure 5a). Ligand deviation analysis (Figure 5b) further supports this, showing that A7OM maintained stability from the start, whereas sitagliptin displayed significant structural deviations. The average ligand RMSD values were 0.58 ± 0.06 nm for A7OM and 0.60 ± 0.33 nm for sitagliptin. Amino acid residue fluctuations (Figure 5c) in both ligand-bound complexes were comparable to the apo-protein, indicating minimal structural perturbations. The mean RMSF scores were 0.09 ± 0.06 nm for A7OM and 0.09 ± 0.079 nm for sitagliptin-bound complexes.

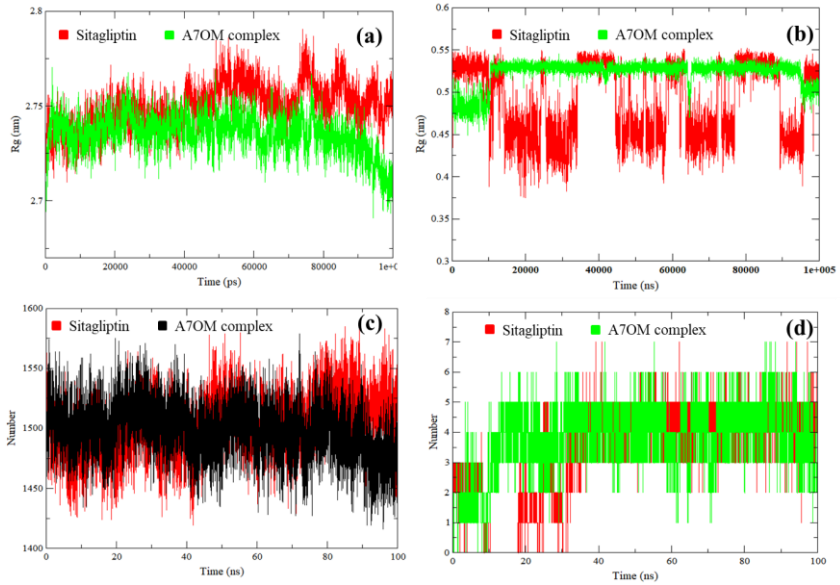

Figure 6. Conformational changes in the DPP4-ligand complexes; (a) Rg of ligand bound complexes, (b) Rg of ligands only, (c) H-bonds between protein and solvent system, and (d) H-bonds between protein and ligands

Figure 6 provides a detailed analysis of the Rg and H-bonds associated with the protein complex and the ligand alone. The Rg value is a critical parameter used in protein structure analysis to assess the compactness of a molecule. In the current study, the Rg value for the A7OM complex was found to be smaller compared to the sitagliptin complex (Figure 6a, b), indicating that the A7OM complex exhibits greater molecular compactness. This observation suggests that the protein-ligand complex adopts a more stable conformation when interacting with the A7OM ligand. The compactness of the structure is further supported by a reduced number of hydrogen bonds (H-bonds) formed between the protein, solvent, and ligand in the A7OM complex (Figure 6c, d). A lower number of H-bonds implies reduced interactions between the protein-ligand complex and surrounding solvent molecules. This reduced interaction may be a result of the tightly packed structure, which not only minimizes solvent accessibility but also contributes to stabilizing the binding of the ligand to the protein. In summary, the smaller Rg value and the reduced number of H-bonds collectively suggest that the A7OM complex forms a more compact and stable structure, which may enhance its binding affinity and reduce susceptibility to solvent interactions compared to the sitagliptin complex. These findings emphasize the importance of structural compactness in the stability and efficacy of protein-ligand interactions. Figure 7 represents the total energy of the protein before and after ligand binding and. The total binding energy of apo-protein i.e., before ligand binding was comparatively higher than that of the both complexes (Figure 7a). The total energy of protein after binding sitagliptin and A7OM was found to be almost similar (Figure 7b, c). The average total energy of Apo protein -A7OM, and sitagliptin complex was found to -14.224x10^5 kcal/mol, -7.654x10^5 kcal/mol and -7.652x10^5 kcal/mol, respectively.

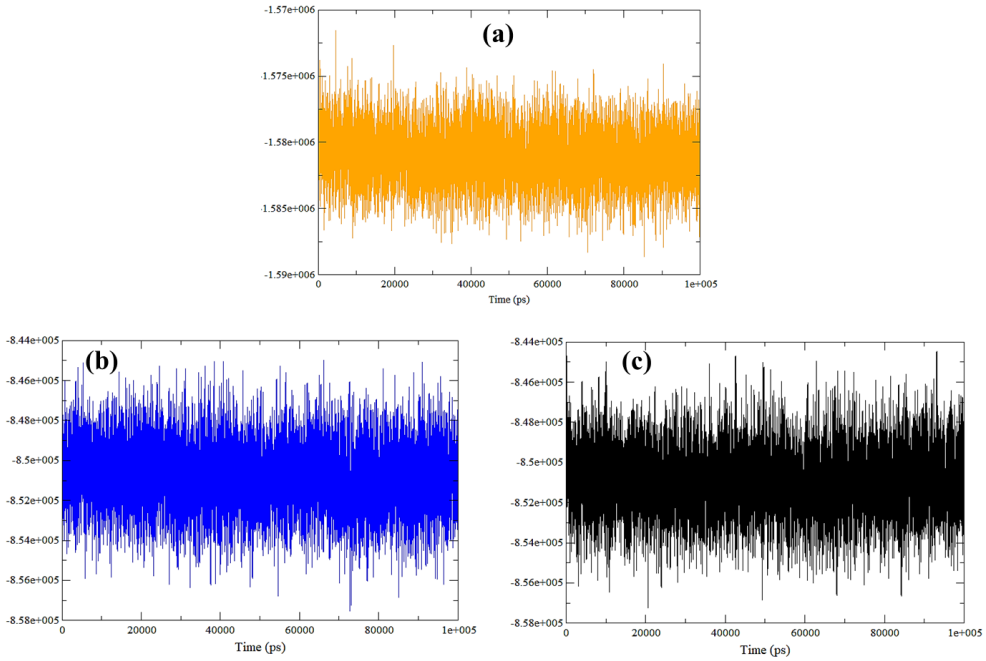

Figure 7. Total energy of (a) DPP4 Apo-protein, (b) DPP4-sitagliptin complex and (c) DPP4-A7OM complex

MM/PBSA analysis

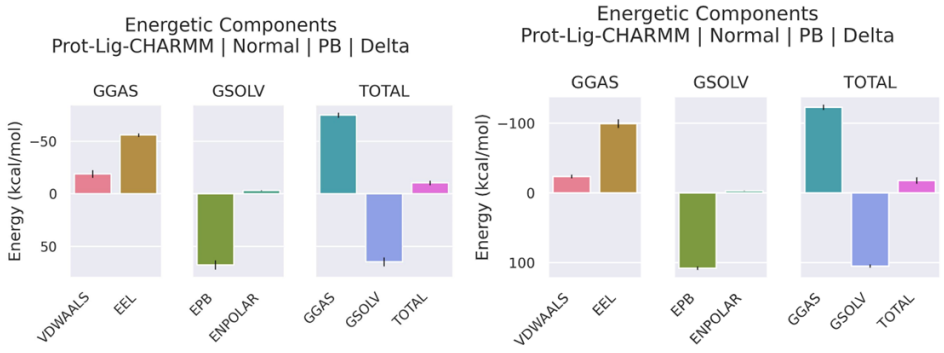

(a) A7OM complex **(b) Sitagliptin complex**

Figure 8. Free energy changes in (a) A7OM-DPP4 complex, (b) apo-protein, (c) ligand (A7OM) and (d) delta values; VDWAALS - van der Waals force, EEL - Electrostatic force, EPB- polar solvation energy, ENPOLsAR - non-polar solvation energy, GGAS- net gas phage energy, GSOLV- net solvation energy

The ligand-bound DPP4 complexes were analyzed further to understand the free energy changes during the simulation (Figure 8). Electrostatic interactions were identified as the primary contributors to binding affinity, followed by Van Der waals interactions. The net gas phase energy (GGAS) during complex formation was approximately -75 kcal/mol, while the net solvation energy (GSOLV) was around 66 kcal/mol, resulting in a total binding energy of approximately -9 kcal/mol. The polar solvation energy (EPB) was estimated at 67 kcal/mol, with the non-polar solvation energy contributing negligibly. These findings highlight the significant role of electrostatic and van der Waals interactions in stabilizing the complex, with solvation effects partially offsetting these favourable interactions.

Discussion

Diabetes mellitus, a chronic metabolic disorder characterized by persistent hyperglycemia, remains a major global health challenge with increasing prevalence (Sun et al., 2022). DPP4-inhibitors are widely used for glycemic control by prolonging incretin activity, enhancing insulin secretion, and reducing glucagon levels (Doupis and Veves, 2008). However, concerns regarding adverse effects, safety, and high costs highlight the need for natural alternatives with better efficacy and safety profiles (Akinyede et al., 2023). Computational approaches like molecular docking, molecular dynamics simulations, and MM/PBSA analysis play a crucial role in identifying potential lead compounds (Kar and Roy, 2021). In the present study, 84 bioactive compounds and four FDA-approved drugs were screened for DPP4 inhibitory activity. Apigenin 7-O-methylglucuronide emerged as the most promising candidate, with 73 bioactive compounds showing stronger binding affinities than the reference drugs. Molecular docking analysis highlighted the importance of structural features such as molecular weight, lipophilicity, and heavy atom count in determining binding affinity. A7OM exhibited superior interactions with the DPP4 active site, consistent with studies showing the inhibitory potential of flavonoids against DPP4 and α-glucosidase (Zhao et al., 2020; Meng et al., 2023). A7OM showed high lipophilicity suggesting improved membrane permeability and bioavailability of the compound (Vistoli et al., 2020).

Molecular interaction analysis revealed that van der Waals interactions were the primary stabilizing force in Sitagliptin, whereas A7OM binding was driven by electrostatic interactions (Kumar et al., 2021). Several flavonoids, including quercetin, luteolin, and kaempferol, exhibit similar structural and functional properties to A7OM (Bhullar et al., 2021; Pradeepa et al., 2023). The phenolic hydroxyl groups of flavonoids contribute to strong hydrogen bonding and electrostatic interactions, enhancing enzyme inhibition (Tanaka et al., 2023). Additionally, flavonoids also provide antioxidant and anti-inflammatory benefits, supporting their role in diabetes management (Afzal et al., 2022). Lipinski's Rule of Five screening showed that while all FDA-approved drugs adhered to the rule, the top five phytochemicals with the highest docking scores violated it due to high molecular weight and excessive hydrogen bond (donors/acceptors). ADMET analysis revealed that Sitagliptin had higher intestinal absorption (0.766) than A7OM (0.323), better blood brain barrier (BBB) penetration (0.961 vs. 0.046), and lower plasma binding affinity (74.85%) compared to A7OM (79.2%), suggesting better therapeutic potential. However, A7OM had a higher LD_{50} (500.18 mg/kg vs. 292.37 mg/kg), indicating lower toxicity.

Molecular dynamics simulations showed that the apo form of DPP4 had higher RMSD values, indicating greater structural flexibility. Ligand binding reduced these fluctuations, enhancing protein rigidity and stability (Hospital et al., 2015). The radius of gyration was lower for the DPP4-A7OM complex, indicating improved compactness and stability (Xu et al., 2019). Hydrogen bonding analysis revealed that the DPP4-A7OM complex had more hydrogen bonds than the DPP4-Sitagliptin complex, attributed to A7OM's higher number of hydrogen bond donors and acceptors (Verma et al., 2022; Ren et al., 2023). MM/PBSA calculations confirmed that the electrostatic interactions played a significant role in DPP4-A7OM binding, while Sitagliptin binding was dominated by van der Waals forces (Kumar et al., 2021; Das et al., 2022). The solvation energy of DPP4-A7OM was positive, indicating reduced solubility but enhanced membrane permeability and bioavailability, as commonly observed in hydrophobic polyphenols (Cheng et al., 2023). This study provides strong computational evidence supporting A7OM as a natural DPP4 inhibitor, with stronger binding affinity, favorable ADMET properties, and enhanced protein stability compared to reference drugs.

Conclusion

The present study identified Apigenin 7-O-methylglucuronide as a promising natural DPP4 inhibitor, exhibiting stronger binding affinity, enhanced stability, and favorable molecular interactions compared to the reference drug, Sitagliptin. Furthermore, molecular docking, MD simulations, and MM/PBSA analysis also confirmed that the phenolic compound, Apigenin 7-O-methylglucuronide stabilized the Dipeptidyl peptidase-4 protein by promoting compactness, with electrostatic and van der Waals interactions playing key roles. Higher hydrogen bonding further supports its strong receptor binding. ADMET analysis suggests good permeability but low solubility, indicating potential formulation needs.

These findings underscore the therapeutic potential of Apigenin 7-O-methylglucuronide in diabetes management. However, future study is needed to focus on *in vitro* and *in vivo* validation, including pharmacokinetics, safety profiles, and possible synergistic effects with existing antidiabetic drugs, to fully explore clinical applicability of Apigenin 7-O-methylglucuronide.

Acknowledgments

Authors acknowledge the Department of Zoology, Bodoland University for providing the necessary facility to carry out the present study.

Author contributions

AS-Design, concept, MD simulation, MM/PBSA analysis, manuscript proofreading; AS- data collection, docking study, manuscript drafting; BN-manuscript drafting, output visualization; KD-MD study, DB-ADMET study, manuscript proofreading.

AI usage declaration

We did not use artificial intelligence in writing this research in any way.

Funding

No funding.

Conflict of interest

The author declares no conflict of interest. The manuscript has not been submitted for publication in other journal.

Ethics approval

NA.

Consent to participate

Not applicable.

Consent to publish

Not applicable.

Data availability statement

All the necessary data for the manuscript are included within the main text, with some additional data provided in the supplementary tables.

References

Abraham, M. J., Murtola, T., Schulz, R., Páll, S., Smith, J. C., Hess, B., & Lindahl, E. (2015) GROMACS: High performance molecular simulations through multi-level parallelism from laptops to supercomputers. *SoftwareX*, *1*, 19-25.

Afzal, M., Kazmi, I., & Mohsin, N. (2022) Flavonoids as potential inhibitors of metabolic disorders: A mechanistic review. *Biomedicine & Pharmacotherapy*, *147*, 112580.

Akinyede, K. A., Adewale, O. S., & Ibrahim, M. A. (2023) Computational approaches in the identification of novel DPP4 inhibitors: A review of recent advances. *Journal of Biomolecular Structure and Dynamics*, *41(5)*, 1125-1140.

Alam, U., Asghar, O., Azmi, S. & Malik, R. A. (2014) General aspects of diabetes mellitus. *Handbook of Clinical Neurology*, *126*, 211-222.

Alberti, K. G., Zimmet, P. & Shaw, J. (2005**)** The metabolic syndrome-a new worldwide definition. *Lancet, 366*, 1059-1062.

Al-Saleh, Y., Sabico, S., Al-Furqani, A., Jayyousi, A., Alromaihi, D., Ba-Essa, E., Alawadi, F., Alkaabi, J., Hassanien, M., Al-Sifri, S., Seham, S., Alessa, T. & Al-Daghri, N. M. (2021) Sulfonylureas in the current practice of type 2 diabetes management: are they all the same? Consensus from the Gulf Cooperation Council (GCC) countries advisory board on sulfonylureas. *Diabetes Therapy*, *12*(8), 2115-2132

American Diabetes Association. (2014) Diagnosis and classification of diabetes mellitus. *Diabetes care*, *37(Supplement_1)*, S81-90.

Bhullar, K. S., Lassalle-Claux, G., & Wu, J. (2021) Bioactive flavonoids as dipeptidyl peptidase IV inhibitors: Therapeutic potential in diabetes management. *European Journal of Pharmacology*, *911*, 174583.

Cheng, H., Lin, X., & Wang, J. (2023) Solubility and permeability of flavonoids: Implications for bioavailability and pharmacokinetics. *Molecular Pharmaceutics*, *20(3)*, 1589-1603.

Das, P., Jha, R. K., & Mohapatra, S. (2022) Molecular docking and MM/PBSA studies of flavonoids as potential inhibitors of DPP4. *Computational Biology and Chemistry*, *102*, 107732.

Deacon, C. F. (2020) Dipeptidyl peptidase 4 inhibitors in the treatment of type 2 diabetes mellitus. *Nature Reviews Endocrinology*, *16*(11), 642-653Y.

Doupis, J. & Veves, A. (2008) DPP4 Inhibitors: a new approach in diabetes treatment. *Advance Therapy*, *25*, 627–643.

Hospital, A., Goñi, J. R., Orozco, M., & Gelpí, J. L. (2015) Molecular dynamics simulations: Advances and applications. *Advances in Protein Chemistry and Structural Biology*, *100*, 77-92.

Hu, F. B., Manson, J. E., Stampfer, M. J., Colditz, G., Liu, S., Solomon, C. G., & Willett, W. C. (2001) Diet, lifestyle, and the risk of type 2 diabetes mellitus in women. *New England journal of medicine*, *345(11)*, 790-797.

Jakubec, D., Skoda, P., Krivak, R., Novotny, M., & Hoksza, D. (2022) PrankWeb 3: Accelerated ligand-binding site predictions for experimental and modelled protein structures. *Nucleic Acids Research*, *50(W1)*, W593–W597.

Kar, S., & Roy, K. (2021) Advances in bioinformatics and computational drug discovery approaches for diabetes mellitus. *Computational Biology and Chemistry*, *94*, 107540.

Khan, C. R. (1994) Insulin action, diabetogenes, and the cause of type II diabetes. *Daibetes*, *43(8)*, 1066-1085.

Kharroubi, A.T. & Darwish, H. M. (2015) Diabetes mellitus: The epidemic of the century. *World journal of diabetes*, *6(6)*, 850.

Kumar, A., Srivastava, A., & Sharma, R. (2021) Molecular insights into flavonoid-DPP4 interactions: A computational approach. *Journal of Biomolecular Structure and Dynamics*, *39(8)*, 2991-3005.

Kumar, A., Srivastava, A., & Sharma, R. (2021) Molecular insights into flavonoid-DPP4 interactions: A computational approach. *Journal of Biomolecular Structure and Dynamics*, *39(8)*, 2991-3005.

Kumari, R., Kumar, R., & Lynn, A. (2014) g_mmpbsa-A GROMACS tool for high-throughput MM-PBSA calculations. *Journal of Chemical Information and Modeling*, *54(7)*, 1951–1962.

Lipinski, C. A. (2004). Lead- and drug-like compounds: The rule-of-five revolution. Drug Discovery Today. *Technologies*, *1(4)*, 337–341.

Meng, X., Zhang, J., & Chen, Y. (2023) Plant-derived polyphenols as DPP4 inhibitors: A structure-activity perspective. *Phytomedicine*, *110*, 154614.

O'Boyle, N. M., Banck, M., James, C. A., Morley, C., Vandermeersch, T. & Hutchison, G. R. (2011) Open babel chemical toolbox. *Journal of Cheminformatics, 3(1),* 33.

Pettersen, E. F., Goddard, T. D., Huang, C. C., Couch, G. S., Greenblatt, D. M., Meng, E. C., & Ferrin, T. E. (2004) UCSF Chimera: A visualization system for exploratory research and analysis. *Journal of Computational Chemistry*, *25(13)*, 1605–1612.

Pires, D. E. V., Blundell, T. L. & Ascher, D. B. (2015) pkCSM: Predicting small-molecule pharmacokinetic and toxicity properties using graph-based signatures. *Journal of Medicinal Chemistry*, *58(9)*, 4066-4072.

Powers, A. C. (2008) Diabetes Mellitus. *Harrison's Principles of Internal Medicine*, *II (17)*, 2275-2304.

Pradeepa, B., Ramesh, N., & Kumari, S. (2023) *In silico* screening of flavonoids for DPP4 inhibition: A computational approach. *International Journal of Biological Macromolecules*, *205*, 196-210.

Robertson, R. P. (1995) Antagonist: diabetes and insulin resistance--philosophy, science, and the multiplier hypothesis. *Journal of Laboratory and Clinical Medicine*, *125(5)*, 560-564.

Sun, H., Saeedi, P., & Karuranga, S. (2022) Global diabetes prevalence estimates for 2021 and projections for 2045: IDF Diabetes Atlas update. *Diabetes Research and Clinical Practice*, *183*, 109119.

Swargiary, A., Daimari, M., Swargiary, A., Biswas, A., Brahma, D. & Singha, H. (2024) Identification of phytocompounds as potent inhibitors of sodium/glucose cotransporter-2 leading to diabetes treatment. *Journal of Biomolecular Structure and Dynamics*, 1-14.

Swinnen, S. G., Hoekstra, J. B. & DeVries, J. H. (2009) Insulin therapy for type 2 diabetes. *Diabetes care*, *32(Suppl 2)*, S253.

Tanaka, T., Takahashi, T., & Shimizu, Y. (2023) Structure-activity relationship studies of flavonoids as DPP4 inhibitors. *Journal of Natural Products*, *86(2)*, 412-428.

Trott, O., & Olson, A. J. (2010) AutoDock Vina: Improving the speed and accuracy of docking with a new scoring function, efficient optimization, and multithreading. *Journal of Computational Chemistry, 31(2)*, 455–461.

Valdés-Tresanco, M. S., Valdés-Tresanco, M. E., Valiente, P. A., & Moreno, E. (2021) gmx_MMPBSA: a new tool to perform end-state free energy calculations with GROMACS. *Journal of chemical theory and computation*, *17(10)*, 6281-6291.

Velan, A., & Hoda, M. (2021) In-silico comparison of inhibition of wild and drug-resistant haemonchus contortus b-tubulin isotype-1 by glycyrrhetinic acid, thymol, and albendazole interactions. *Journal of Parasitic Diseases: Official Organ of the Indian Society for Parasitology*, *45(1)*, 24–34.

Verma, R., Singh, S., & Yadav, M. (2022) Computational pharmacokinetics and ADMET profiling of flavonoids as DPP4 inhibitors. *Chemico-Biological Interactions*, *365*, 110014.

Vistoli, G., Pedretti, A., & Testa, B. (2020) Assessing drug-likeness: Lipophilicity, solubility, and permeability. *Future Medicinal Chemistry*, *12(10)*, 813-828.

Xiong, G., Wu, Z., Yi, J., Fu, L., Yang, Z., Hsieh, C., & Cao, D. 2021 ADMETlab 2.0: an integrated online platform for accurate and comprehensive predictions of ADMET properties. *Nucleic Acids Research*, *49(W1)*, W5-W14

Xu, L., Wu, J., & Zhao, W. (2019) Stability and interaction mechanisms of polyphenol-protein complexes: A molecular dynamics study. *Food Chemistry*, *293*, 328-337.

Yang, Y., Shi, C. Y., Xie, J., Dai, J. H., He, S. L., & Tian, Y. (2020) Identification of potential dipeptidyl peptidase (DPP)-IV inhibitors among *Moringa oleifera* phytochemicals by virtual screening, molecular docking analysis, ADME/T-based prediction, and *in vitro* analyses. *Molecules*, *25(1)*, 189.

Zhao, H., Song, L., & Li, Z. (2020) Flavonoids as potential inhibitors of α-glucosidase and DPP4: Implications for diabetes therapy. *European Journal of Medicinal Chemistry*, *198*, 112402.

Zoete, V., Cuendet, M. A., Grosdidier, A., & Michielin, O. (2011) SwissParam, a fast force field generation tool for small organic molecules. *Journal of Computational Chemistry*, *32(11)*, 2359–2368.